

CONTACTLESS MAGNETIC MICRO-BEARING APPLIED TO ELECTROSTATIC INDUCTION MICROMACHINES

Y. D. Valencia, J. M. Monzón-Verona, S. García-Alonso
Institute for Applied Microelectronics (IUMA)
Dept. of Microelectronics and Microsystems (MEMS)
University of Las Palmas de Gran Canaria (ULPGC), Spain

Abstract: This paper presents the design and analysis of four magnetic microbearings applied to micro electrostatic induction machines. We have considered four models with different measures. We have conducted an analysis by the finite element method using Magnetic Fem program. Furthermore, an analysis of the tangential and normal stresses has been carried out.

Keywords: magnetic microbearings, micromachines, free friction, micromotor, MEMS.

I. INTRODUCTION

Micromotors [3] are devices employing electrical, mechanical or chemical and make it move. They are devices that are manufactured to millimeter scales, which are related to everything that encompasses MEMS. These manufacturing systems must be developed on a stand that allows to have zero friction, making the following advantages:

- Less wear use
- Very high speeds and high stability.

The micromotors are classified into electrical, chemical and mechanical. They have applications in medicine and engineering, among others. It is important to understand magnetic microbearings as this article will address the design and analysis of one of them [5].

A magnetic bearing [7] is any microbearings based on magnetic effects to achieve mechanical drive device. What differentiates the magnetic bearings is their size, since they are limited to sizes typically measured in microns up to about one or two mm in overall size. Moreover, the friction has been a limiting factor in its successful development and for use in various applications micromachines factor. One approach to alleviate this problem is to use techniques such as magnetic microbearings magnetic suspension. In magnetic bearings [9] the suspension forces are generated magnetically without any contact. Due to the contact low friction, the magnetic bearings can be used to achieve high rotational speeds. Besides other advantages of magnetic microbearings are low maintenance, no need for lubrication and longer life expectancy. Some categories [3] which belong to the magnetic microbearings are presented below:

1. Interaction of a conductor moving in a magnetic field. This is subject to the Lorentz force.
2. Interaction of a conductor and an AC voltage. Levitation of a drop of molten metal is an example.
3. Interaction of the field of a permanent magnet and a conductor. This can be used by an active magnetic bearing.
4. Diamagnetic bearings. Based on the diamagnetic effect of the materials such as bismuth or graphite. The effect is weak, therefore, applications are limited to small masses or passive stabilization bearings, where the weight is compensated by the permanent magnets.
5. The bearings are based on superconducting materials. This type is essentially due to the relative permeability of superconductors. It is a kind of force amplified with a diamagnetic effect.

II. DESIGN AND ANALYSIS OF A MAGNETIC MICROCOJINETE USED IN ELECTROSTATIC INDUCTION MICROMACHINES

Two magnetic microbearings were designed, one asymmetrical and one symmetrical, with different measures. Both were analyzed. First we present the asymmetrical magnetic microbearings.

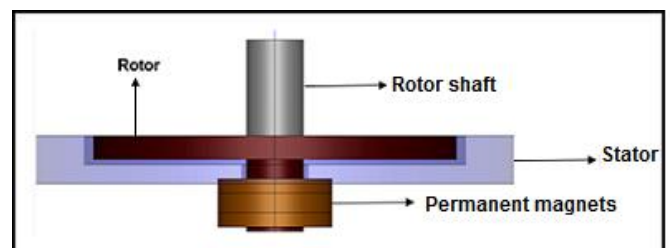


Fig.1 Asymmetric magnetic bearing

This design has four permanent magnets, two in the rotor and two the stator. To make it more stable and avoid additional problems a symmetric magnetic microbearings was designed.

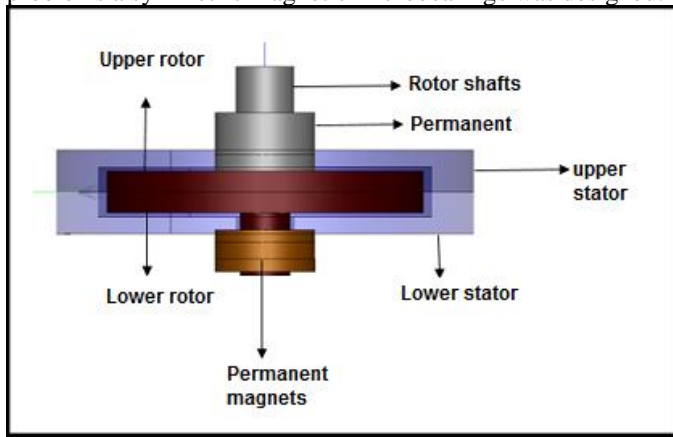


Fig.2 Symmetric magnetic bearing

III. ANALYSIS AND NORMAL TANGENTIAL STRESSES

Some experimental parameters for the design of electrostatic induction micromotor electric [6] were taken, as can be seen in the following table.

Table I Values taken to calculate the torque and normal force

Parameter	Sign	Design	Unit
Voltage applied to the stator	V	285	V
Excitation frequency of the stator	f	2.6	MHz
Stator frequency	m	131	--
Air gap between rotor space	G	3	μm
Resistance of conductor layer	Pres	200	M Ω
Rotor speed synchronous	Ω	1.2×10^6	rpm
Insulations thickness of the rotor	Ari	10	μm
Inner radius of the rotor conductor	Ri	1	mm
Outer radius of the rotor conductor	Ro	2	mm
Rotor insulations resistivity	Pri	1.0×10^{14}	$\Omega\text{-cm}$

To calculate the tangential force and the normal force the following formulas were used, based on the article [6] for the tangential force:

$$\tau = \int_{R_i}^{R_o} r \omega f \gamma \omega \cdot 2\pi r dr = \omega \varepsilon g \pi V^2 \int_{R_i}^{R_o} \alpha(r) \beta(r) \chi(r) dr$$

where

$$\alpha(r) = \frac{\Gamma(r)}{1 + \Gamma(r)^2}$$

$$\beta(r) = \frac{\varepsilon g}{\varepsilon_{eff}(r) \omega \sinh(\frac{mG}{r})}$$

and

$$\chi(r) = \frac{m^2}{\sinh(\frac{m}{r}G)}$$

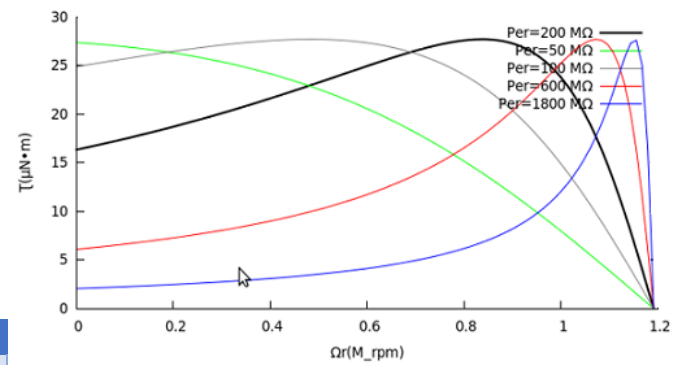


Fig.3 Sensitivity analysis of the torque versus rotor speed

Normal force is given by the following formula:

$$\tau = \int_{R_i}^{R_o} f z \cdot 2\pi r dr = \varepsilon g 2\pi \int_{R_i}^{R_o} \alpha(r)^2 \beta(r) dr$$

where

$$\alpha(r)^2 = \left[\frac{\frac{m}{r} V}{2 \sinh(\frac{m}{r} G)} \right]^2$$

and

$$\beta(r) = 1 + \Gamma^2 \cdot \frac{\left[\left(\frac{\varepsilon g}{\varepsilon_{eff}(r) \sinh(\frac{m}{r} G)} \right)^2 - 2 \cdot \left(\frac{\varepsilon g}{\varepsilon_{eff}(r) \sinh(\frac{m}{r} G)} \right) \cdot \cosh(\frac{m}{r} G) + 1 \right]}{1 + \Gamma^2}$$

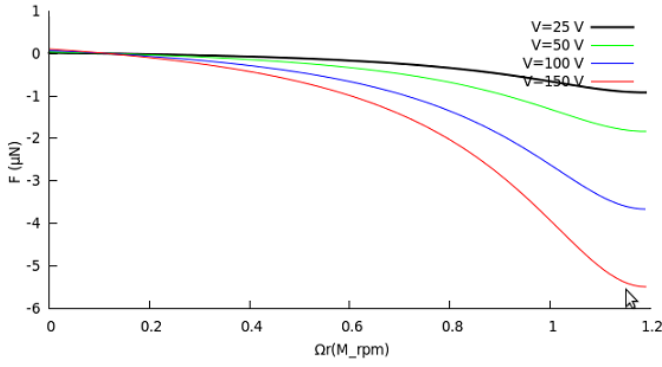


Fig. 4 Sensitivity analysis of the torque versus the stator amplitude voltage

Fig.4 shows that when use change the amplitude of the stator voltage, from 0.19 μN presents an attractive force that increases as the voltage amplitude of the stator increases. Initially with a value of 25 V it has an attraction strength that takes a value of -0.91 μN . In addition, when it takes a value of 150 V, the attractive force is greater with -5.47 μN .

IV. STIFFNESS CALCULATION OF MAGNETIC AND DIELECTRIC

The magnetic stiffness and the dielectric for magnetic microbearings calculated. The following table shows the values generated for each of the models. It is observed how as the size of the model increases, the stiffness increases, presenting model N.4 a greater stiffness value with 1.86 $\mu\text{N}/\mu\text{m}$.

Table II Stiffness of magnetic microbearings for negative offset

Model	Force	Displacement (z)	Magnetic Rigidity
1	1.66 mN	2 μm	0.83 mN/ μm
2	2.32 mN	2 μm	1.16 mN/ μm
3	3.54 mN	2 μm	1.77 mN/ μm
4	3.72 mN	2 μm	1.86 mN/ μm

Moreover, we calculated dielectric k_i for each model. This rigidity is calculated using the following formula.

$$k_s = \frac{Fz}{I}$$

Where F is the force generated and I is the current used. The dielectric strength resulted in a value of:

$$k_i = \frac{2}{0.3} = 6.66 \mu\text{N}/\text{A}$$

V. ANALYSIS OF A MAGNETIC MICROCOJINETE BY FINITE ELEMENT METHOD

To perform this analysis, two models with different sizes, were used, each with a different measures

1. The first model is 80 x 40 x 40 μm . It also has two permanent magnets 10 x 30 μm , one at the top and one at the bottom. Also in the center has a division 10 x 20 μm in which the aluminum is located.
2. The second model is 120 x 60 x 60 μm . Like the previous model, it has two permanent magnets 20 x 50 μm , one at the top and one at the bottom. In the center it also has a division of 20 x 20 μm in which aluminum is located.
3. The third is 140 x 90 x 90 μm , like the previous model, it has two permanent magnets 50 x 30 μm , one at the top and one at the bottom. Also in the center has a division 40 x 30 μm in which aluminum is located.
4. The fourth is 140 x 90 x 120 μm . Like the previous model, it has two permanent magnets 50 x 30 μm one at the top and one at the bottom. Also in the center has a division 40 x 30 μm in which aluminum is located.

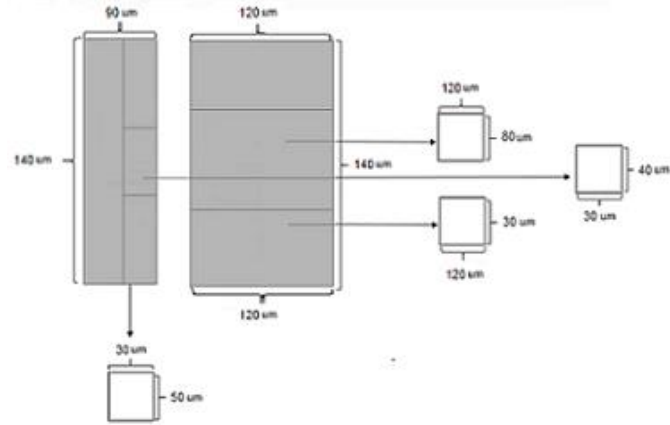


Fig.5 Dimensions of the proposed design for the model N. 4

This fourth model has much larger dimensions, which allows to locate in a particular area (central part of the right microcojinet) a large number of coils, which in this case are 19, features 4 NdFeB permanent magnets 32 MGOe. In addition to aluminum and the air then exit geometry for this design is observed.

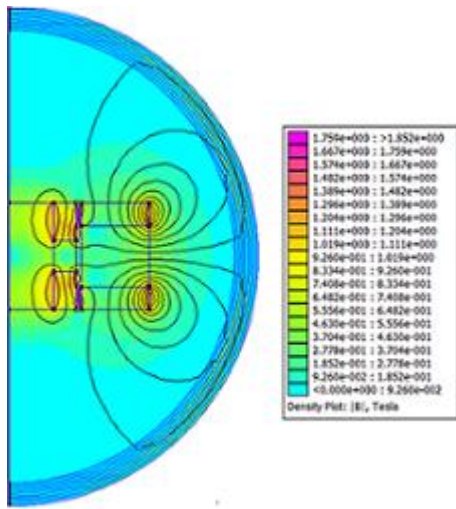


Fig.6 Plot of flux density

The previous figure shows that the force focuses mainly on the four permanent magnets and has a lower flux density in the corners, both above and below. For this analysis a current of 0.3 A was applied, and a gap of 2 μm was taken. The chart below shows each of the simulations using a certain number of coils with a space of 2 μm . It is dear again that we should use the maximum number of coils as it allows more room for regulation. Unlike the simulation using the aluminum, this presents a larger space as a number of short rolls 19 at 0.5 μm , while the court in aluminum is 0.36 μm .

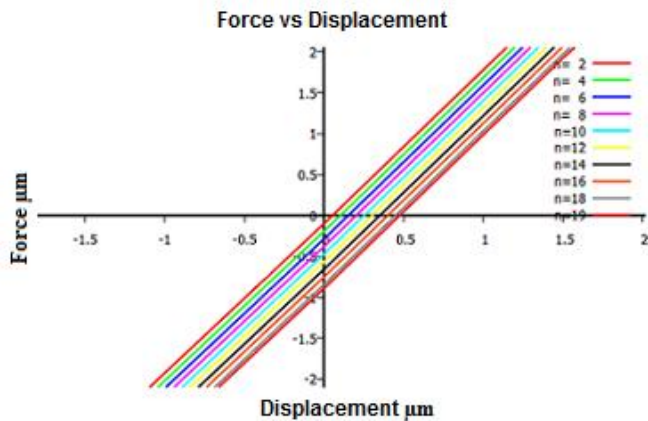


Fig.7 Relationship between force and displacement using iron model N.4

IV. RESULTS OBTAINED

When analyzing the tangential and normal stresses we observed that the growth of the rotation speed in the tangential force is influenced by the resistance of the conductive layer and those having a higher resistance value in this pair exhibit reduced. Furthermore it is observed that the smaller resistance values are those having a greater starting torque. Moreover the

values of the resistor layer tangency rotation force couple have on equal maximum.

When performing the analysis by the finite element method it is observed how it influences the diameter of each model, both in the number of coils and diameter of regulation. The following table shows the amount of coils calculated for each of the models proposed

Since current influences when making simulations and not recommended a higher current to 0.3A and based on the article [2] was found to use the number of coils to avoid the need to increase more current and thus correct the disturbances that arise.

Table III Number of coils for each surface

Model	Measures	Number of coils
1	40 μm x 40 μm	3
2	60 μm x 60 μm	7
3	80 μm x 90 μm	14
4	80 μm x 120 μm	19

It is noteworthy that the force in relation to the movement is also influenced by the model when movement occurs. The model No. 4 is optimal and generates better results when performing the simulations. On the other hand it is also observed that using such conductive member benefits more iron than aluminum for the same reason as mentioned above.

V. CONCLUSIONS

- The design of two mixed symmetric and asymmetric magnetic microcojinete is presented.
- Analysis of the tangential and normal stresses greater influence was performed and observed by the resistance of the conductive layer, on the other hand, those who have an increased resistance value is shown in a lower starting torque and vice versa.
- It is noted that the values of the resistance layer tangency rotation force couple have an equal maximum.
- Sensitivity analysis using the finite element method is performed, it is observed as the size of the model influence and improves regulation of micromotor space, as far as it has more room to regulate.
- When calculating the magnetic stiffness it is observed that this also increases as the size increases in the model coming to take values from 0.75 mN / μm to 1.82 mN / μm .

- When performing the sensitivity analysis using as conductive element iron shows that have a greater regulatory space so it is best to use the conductive element. Moreover it is observed that using both aluminum and iron at the time of plotting flux density induced currents are mainly focused on the region where these elements.

REFERENCES

- [1] Assadsangabi, B., M. Tee, and K. Takahata (2013, June). Ferrofluid-assisted levitation mechanism for micromotor applications. In Solid-State Sensors, Actuators and Microsystems (TRANSDUCERS EUROSENSORS XXVII), 2013 Transducers Eurosensors XXVII: The 17th International Conference on, pp. 2720_2723.
- [2] Badilita, V., K. Kratt, T. Burger, J. Korvink, and U. Wallrabe (2009, June). 3d high aspect ratio, mems integrated micro-solenoids and helmholtz microcoils. In Solid-State Sensors, Actuators and Microsystems Conference, 2009. TRANSDUCERS 2009. International, pp. 1106 1109.
- [3] Ghalichechian, N., A. Modafe, M. Beyaz, and R. Ghodssi (2008, June). Design, fabrication, and characterization of a rotary micromotor supported on microball bearings. *Microelectromechanical Systems, Journal of* 17 (3), 632 642.
- [4] Jayawant, B. V. (1981). Electromagnetic suspension and levitation. *Reports on Progress in Physics* 44 (4), 411.
- [5] Lang, J. and S. Bart (1988, jun). Toward the Design of Successful Electric Micromotors. In Solid-State Sensor and Actuator Workshop, 1988. Technical Digest. IEEE, pp. 127 130.
- [6] Nagle, S., C. Livermore, L. Frechette, R. Ghodssi, and J. H. Lang (2005, Oct). An electric induction micromotor. *Microelectromechanical Systems, Journal of* 14 (5), 1127 1143.
- [7] Schweitzer, G., H. Bleuler, E. H. Maslen, M. Cole, P. Keogh, R. Larssonneur, E. Maslen, Y. Okada, G. Schweitzer, A. Traxler, et al. (2009). *Magnetic bearings: theory, design, and application to rotating machinery*. Springer.
- [8] Wilkinson, S. G., P. Mellor, and D. Holliday (2004, Sept). Design of a magnetic bearing for high speed rotating micro-machines. In Universities Power Engineering Conference, 2004. UPEC 2004. 39th International, Volume 2, pp. 570 574 vol. 1.
- [9] Wong, W., W. K. S. Pao, D. Holliday, and P. Mellor (2006, Oct). Design and modeling of an electromagnetic levitated and actuated micromotor. In Semiconductor Electronics, 2006. ICSE '06. IEEE International Conference on, pp. 309 313.